

Atom trapping in deeply bound states of a far-off-resonance optical lattice

D. L. Haycock, S. E. Hamann, G. Klose, and P. S. Jessen
Optical Sciences Center, University of Arizona, Tucson, Arizona 85721
 (Received 20 December 1996)

We form a one-dimensional optical lattice for Cs atoms using light tuned a few thousand linewidths below atomic resonance. Atoms are selectively loaded into deeply bound states by adiabatic transfer from a superimposed, near-resonance optical lattice. This yields a mean vibrational excitation $\bar{n} \approx 0.3$ and localization $\Delta z \approx \lambda/20$. Light scattering subsequently heats the atoms, but the initial rate is only of order 10^{-3} vibrational quanta per oscillation period. Low vibrational excitation, strong localization, and low heating rates make these atoms good candidates for resolved-sideband Raman cooling. [S1050-2947(97)50706-2]

PACS number(s): 32.80.Pj, 42.50.Vk

The ac Stark shift (light shift) arising in laser interference patterns can be used to create stable periodic potentials for neutral atoms. Under appropriate conditions these ‘‘optical lattices’’ will laser cool and trap atoms in individual optical potential wells, with center-of-mass motion in the quantum regime. Experiments have explored a number of such lattice configurations in one, two, and three dimensions, and detailed insight into the dynamics of cooling and trapping has been gained through probe absorption and fluorescence spectroscopy [1]. The possibility of atomic confinement deep in the Lamb-Dicke regime suggests that it is worthwhile to pursue schemes for resolved-sideband Raman cooling [2] and quantum-state preparation [3], as recently demonstrated for trapped ions.

In a standard optical lattice formed by near-resonance light, control of the center-of-mass motion is limited by rapid laser cooling and heating processes that occur at a rate determined by photon scattering. These dissipative processes are readily avoided when the lattice is formed by intense light tuned far from atomic transition. Such far-off-resonance lattices have been used extensively in atom optics as diffraction gratings and lenses [4] and as model systems in which to study quantum chaos [5] and quantum transport [6]. When far-off-resonance optical lattices are used to trap atoms, however, the absence of built-in laser cooling makes it difficult to obtain vibrational excitation and confinement comparable to the near-resonance case. Accordingly, experiments on far-off-resonance lattices have so far achieved low vibrational excitation only by allowing the majority of vibrationally excited atoms to escape [7]. We demonstrate here a loading scheme, in which cesium atoms are first cooled and trapped in a near-resonance lattice, and then adiabatically transferred to a superimposed far-off resonance lattice. Immediately following transfer we achieve trapping parameters comparable to the near-resonance case, with a mean vibrational excitation as low as $\bar{n} \approx 0.3$, and a typical rms position spread of $\Delta z \approx \lambda/20$. Based on the lattice parameters we calculate an off-resonance photon scattering rate of order 10^3 s^{-1} . We find, however, that Lamb-Dicke suppression of spontaneous Raman scattering keeps the accompanying increase in vibrational excitation on the order of 10^{-3} quanta per oscillation period. Heating is therefore almost negligible on vibrational time scales.

We form our far-off-resonance optical lattice using a pair of counterpropagating laser beams of linear and orthogonal polarizations [the one-dimensional (1D) lin \perp lin configuration [1]], tuned a few tens of GHz below the $6S_{1/2}(F=4) \rightarrow 6P_{3/2}(F'=5)$ transition at $\lambda=852 \text{ nm}$. The lattice beams are produced with a 0.5-W single-mode diode laser; this limits the peak intensity to 1 W/cm^2 for Gaussian lattice beams with an intensity full width at half maximum $\approx 3.3 \text{ mm}$. The 1D lin \perp lin configuration creates a pair of $\sigma+$ and $\sigma-$ polarized standing waves, offset by $\lambda/4$ so that the antinodes of one standing wave coincide with the nodes of the other. In the limit of weak excitation the lattice potential for the ground hyperfine state $|F, m\rangle$ is the sum of the light shifts associated with driven transitions to states $|F', m'\rangle$ in the excited-state manifold,

$$U_{Fm}(z) = \frac{\hbar\Gamma}{8E_R} \frac{I}{I_0} \sum_{F'm'} \frac{\Gamma}{\Delta_{F'}} f_{Fm}^{F'm'} [(m' - m)\cos(2kz) + 1]. \quad (1)$$

In this expression $\Gamma = 2\pi \times 5.22 \text{ MHz}$ is the natural linewidth, $E_R = (\hbar k)^2/2m$ is the photon recoil energy, I is the intensity per lattice beam, $I_0 = \pi\hbar\Gamma c/3\lambda^3 = 1.10 \text{ mW/cm}^2$ is the saturation intensity, $\Delta_{F'}$ is the detuning from the $F \rightarrow F'$ transition, and $f_{Fm}^{F'm'}$ is the oscillator strength for the transition $|F, m\rangle \rightarrow |F', m'\rangle$. In the far-off-resonance limit Eq. (1) yields a set of potentials that is topographically similar to the potentials associated with an isolated $F=4 \rightarrow F'=5$ transition, with potential minima located at sites of pure $\sigma+$ ($\sigma-$) polarization for states $|4, m > 0\rangle$ ($|4, m < 0\rangle$). In this work we are interested in states localized near the potential minima, where the diabatic and adiabatic potentials (obtained by diagonalizing the light-shift Hamiltonian) are indistinguishable. In that case we can approximate the atoms by product states $|4, m, n\rangle = |4, m\rangle \otimes |n_m\rangle$, where $|n_m\rangle$ is an eigenstate of the anharmonic oscillator obtained by expanding the diabatic potential $U_{4m}(z)$ to order $(kz)^4$ around a potential minimum. Exceptions are states involving the magnetic sublevel $|4, 0\rangle$, which are unbound; in our experiment those states contain less than 5% of the total population and can be ignored.

We load this far-off-resonance lattice with atoms from a superimposed 1D lin \perp lin near-resonance lattice. A cycle of

our experiment proceeds as follows. A cold ($3\text{-}\mu\text{K}$, 10^{10}-cm^{-3}) sample of Cs atoms is produced using a standard vapor cell magneto-optical trap (MOT) and 3D optical molasses. The MOT-3D molasses beams are extinguished and the atoms equilibrate in the near-resonance lattice for ≈ 1 ms, during which time they are optically pumped into the magnetic sublevels $|4, m = \pm 4\rangle$ and become trapped in the few lowest vibrational states of the corresponding lattice potential wells. Transfer to the far-off-resonance lattice is accomplished by a simultaneous linear turn-off and turn-on of the near- and far-off-resonance potentials over a $\approx 200\text{-}\mu\text{s}$ period. During the MOT-3D molasses and near-resonance lattice phases a separate laser provides repumping from the $6S_{1/2}(F=3)$ hyperfine ground state; this repumping laser is not present during the far-off-resonance lattice phase.

The axes of the near- and far-off-resonance lattices are parallel and vertical to better than 20 mrad, and we use time-of-flight analysis to measure the momentum distribution in both. This is accomplished by suddenly releasing the atoms from the lattice and measuring the distribution of arrival times as they fall through a $\approx 200\text{-}\mu\text{m}$ -thick horizontal sheet of probe light located 5 cm below the lattice volume. Our setup can detect atoms trapped in the lattice for times $\tau \leq 100$ ms. However, at times $\tau \gtrsim 5$ ms motion transverse to the lattice axis causes the atom cloud to expand significantly into the wings of the Gaussian lattice beams. The transverse motion into shallower potentials leads to adiabatic cooling [1], and the momentum distribution is narrowed accordingly. As described below, this must be taken into account when the momentum spread is used to determine vibrational excitation and localization. Adding a magnetic field gradient and bias field as the atoms fall from the lattice to the probe volume permits us to separate arrival times, and to measure populations for the magnetic sublevels $|4, m\rangle$ [8].

To achieve low vibrational excitation and strong localization one must load atoms selectively into deeply bound states. In principle, this can be accomplished if atoms are adiabatically released from a near-resonance lattice and then recaptured in a superimposed far-off-resonance lattice. During adiabatic release and recapture the tightly bound states in the near-resonance lattice evolve into free-particle states of near-zero momentum and then into tightly bound states of the far-off-resonance lattice [1]. This type of adiabatic transfer should work well even if the near- and far-off-resonance lattices have slightly different lattice constants or symmetry. In our setup, however, it fails for several reasons. Most importantly the presence of gravity precludes adiabatic evolution via free states, as unbound atoms are quickly accelerated away from zero momentum. In addition, residual magnetic fields will cause precession of the atomic spin in the absence of lattice light, and change the distribution of population over magnetic sublevels. A similar change in the atomic internal state can occur if the transfer between lattices is non-adiabatic with respect to the atomic internal degrees of freedom. It may be possible to overcome these difficulties by transferring the atoms in a free-falling frame, and in the presence of a bias magnetic field along the lattice axis.

In this work we instead keep the atoms strongly localized in deep potential wells at all times. This is accomplished by overlapping the potential wells of the near- and far-off-resonance lattices, and by coordinating the turn-on and turn-

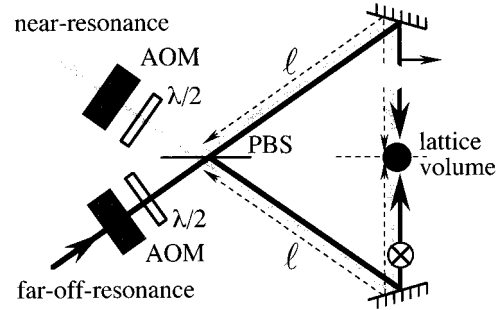


FIG. 1. Experimental setup for adiabatic transfer between lattices. Near- and far-off-resonance laser beams are combined with a polarization beam splitter (PBS). Pairs of acousto-optic modulators (AOM) and half-wave plates ($\lambda/2$) provide independent control of the intensities of the two pairs of lattice beams. Equal optical path lengths ℓ from beam splitter to atomic sample (to better than 1 mm) ensure that the lattice potential wells remain adequately overlapped, as long as the lattice frequency difference is well below 150 GHz.

off of the lattices so the sum of the potentials remains approximately constant during the transfer. Good overlap between the potential wells of the near- and far-off-resonance lattices is critical, and is accomplished as illustrated in Fig. 1.

The momentum distribution of a sample of atoms in the near- or far-off-resonance lattice [Fig. 2(a)] is indistinguishable from a Gaussian fit, from which we obtain the rms momentum Δp . Based on a few reasonable working assumptions we can then obtain information about the populations π_{mn} of the states $|4, m, n\rangle$ by setting $\Delta p^2 = \langle \sum_{m,n} p_{mn}^2 \pi_{mn} \rangle$, where p_{mn}^2 is the mean-square momentum in state $|4, m, n\rangle$, and the average is performed over the distribution of atomic positions in the lattice. We first assume that π_{mn} does not depend strongly on position and also that the distribution of population over the vibrational states $|n_m\rangle$ is nearly independent of $|m\rangle$. In this approximation $\Delta p^2 \approx \sum_{m,n} \langle p_n^2 \rangle \pi_n$, where $\langle p_n^2 \rangle$ is the mean-square momentum for the manifold

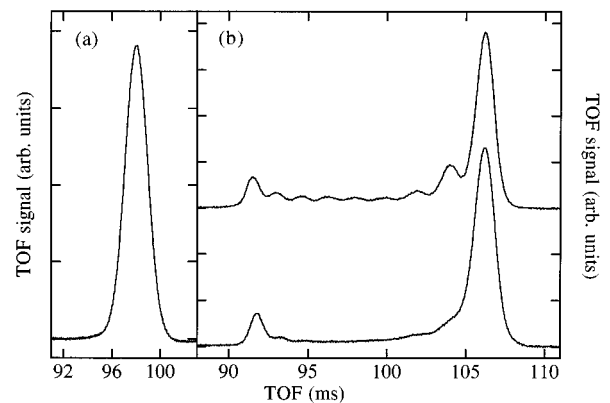


FIG. 2. (a) Typical time-of-flight distribution measured for atoms in the far-off-resonance lattice. The corresponding momentum distribution is indistinguishable from a Gaussian. (b) Time-of-flight distribution in the presence of a gradient magnetic field, for the near- (lower curve) and far-off-resonance (upper curve) lattices. Each of the nine peaks corresponds to atoms in a separate magnetic sublevel.

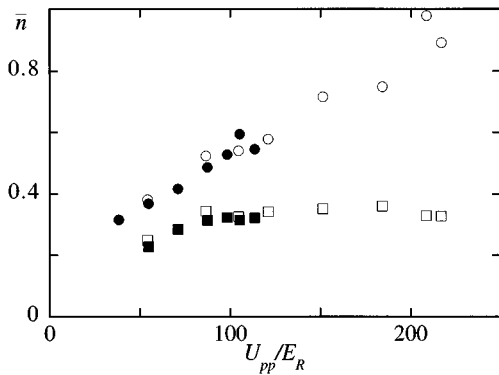


FIG. 3. Mean vibrational excitation \bar{n} in the far-off-resonance lattice, as a function of the peak-peak modulation depth U_{pp} of the lattice potential U_{44} . Solid (open) symbols indicate data taken for lattice detunings of $\Delta = -20$ GHz ($\Delta = -10$ GHz). Circles (squares) indicate vibrational excitation measured at $\tau = 20$ ms ($\tau = 0.1$ ms) after transfer from the near-resonance lattice.

$\{|n_m\rangle\}$ of the n th excited vibrational states, averaged over position and weighted by the populations of the $|4, m\rangle$ states, and $\pi_n = \sum_m \pi_{nm}$ is the total population of the manifold $\{|n_m\rangle\}$. We then assume a thermal distribution over vibrational states, and calculate the vibrational temperature that yields the observed Δp . Finally we use the mean excitation $\bar{n} = \sum_n n \pi_n$ as a convenient measure to describe the degree of vibrational excitation.

We precool and localize atoms in a near-resonance lattice with intensity $I = 2.5I_0$ per beam and detuning $\Delta = -23\Gamma$. This corresponds to a peak-peak modulation depth $U_{pp} = 78E_R$ of the $U_{44}(z)$ diabatic potential, with three bound states in each potential well for the $|4, m = \pm 4\rangle$ states. Figure 2(b) shows a time-of-flight distribution with individual states $|4, m\rangle$ separated by a gradient magnetic field; the corresponding population of the states $|4, m = \pm 4\rangle$ is ~ 0.75 . The evident population asymmetry between states $|4, m = 4\rangle$ and $|4, m = -4\rangle$ most likely derives from imperfect lattice polarization or from a nonzero magnetic field parallel to the lattice axis [9]. From the measured momentum spread $\Delta p = (2.57 \pm 0.04)\hbar k$ we infer an $\bar{n} = 0.37 \pm 0.03$ [10], corresponding to a population of the vibrational ground-state manifold of $\pi_0 = 0.73$. Taking into account the population in states $|4, m = \pm 4\rangle$ we estimate a population $\pi_{\pm 40} \approx 0.55$ in the lowest bound state of the lattice.

To show that our transfer scheme results in negligible heating we measure \bar{n} immediately after transfer, for different values of the lattice depth U_{pp} and detuning Δ from the $F = 4 \rightarrow F' = 5$ transition (Fig. 3). For lattices that are not too shallow we find $\bar{n} = 0.34 \pm 0.03$ [10]. Using a thermally excited anharmonic-oscillator model we calculate the rms localization to be in the range $\lambda/17 - \lambda/24$, depending on lattice depth. These initial values are comparable to those achieved in near-resonance lattices. A measurement of the distribution of population over states $|4, m\rangle$ [Fig. 2(b)] shows that the magnetization is slightly less than in the near-resonance lattice, with a total population of ~ 0.55 in states $|4, m = \pm 4\rangle$. Transfer efficiency between the near- and far-off-resonance lattices is typically in the range 90–95 %.

Atoms in the far-off-resonance lattice are slowly heated by photon scattering. Figure 4 shows the increase in

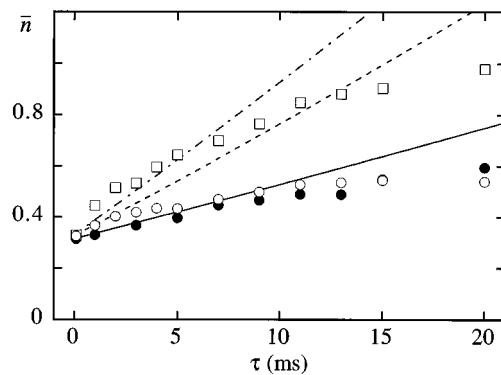


FIG. 4. Mean vibrational excitation \bar{n} in the far-off-resonance lattice, as a function of time τ elapsed since transfer from the near-resonance lattice. Solid circles correspond to a lattice detuning $\Delta = -20$ GHz (-3831Γ) and a peak-peak modulation length $U_{pp} = 105E_R$ of the U_{44} potential. Open symbols correspond to $\Delta = -10$ GHz (-1916Γ) and $U_{pp} = 105E_R$ (circles), $U_{pp} = 209E_R$ (squares). Solid, dashed, and dot-dashed lines show the expected heating from photon scattering.

\bar{n} , as a function of trapping time τ , for lattices of different depth and detuning. We note that our measurement of \bar{n} becomes less reliable as τ increases. This happens partly due to uncertainty about the transverse velocity of the atoms, but mostly due to a breakdown of the anharmonic-oscillator model as atoms heat up and as they move into regions of shallow potentials. For comparison, a band-structure calculation for $U_{pp} = 105E_R$ and $U_{pp} = 209E_R$ (corresponding to Fig. 4) shows 3 and 5 bound states, respectively, in the wells of the $U_{44}(z)$ potential. We estimate that the uncertainty on \bar{n} is $\pm 10\%$ at $\tau \sim 0$ ms, increasing to $\pm 20\%$ at $\tau = 20$ ms [10]. Accordingly, we do not show values for times $\tau > 20$ ms, even though a time-of-flight signal is easily detectable.

Initially \bar{n} increases roughly as expected from photon scattering. For an atom localized near an antinode of the $\sigma+$ standing wave and optically pumped into the state $|4, m = 4\rangle$, the scattering rate is close to $\gamma_s = \Gamma(I/4I_0)/(\Delta/\Gamma)^2$. For the parameters of Fig. 4 this corresponds to photon scattering rates in the range $\gamma_s = 500 - 2000 \text{ s}^{-1}$. Figure 4 shows calculations of \bar{n} vs time, obtained by solving rate equations for the vibrational populations for an atom bound in a potential well of the $U_{44}(z)$ optical potential, on the axis of the lattice beams. A more quantitative comparison with theory is not attempted here, and will be difficult to accomplish given the uncertainty on \bar{n} at long trapping times. Irrespective of the details of the model, however, one always expects the rate of heating to increase with the photon scattering rate. Figure 4 shows this dependence only during the first few milliseconds; at later times \bar{n} depends only on the lattice depth. Figure 3 illustrates this linear scaling of \bar{n} with lattice depth, at $\tau = 20$ ms. This behavior is qualitatively similar to the steady-state scaling known from near-resonance lattices [1], and one might speculate that a cooling mechanism is active also in the far-off-resonance case. Unfortunately the limited interaction time available in our 1D geometry does not permit us to confirm or rule out whether \bar{n} will eventually reach steady state.

It is possible that the increase in \bar{n} is limited by the escape

of atoms with a thermal energy above the lattice potential-well depth. We find that the number of atoms trapped in the lattice decays exponentially, with a time constant $\tau_0 \approx (2 \text{ ms/GHz}) \times \Delta$. This scaling is consistent with loss caused predominantly by the escape of hot atoms. An atom trapped in a potential well of depth U_{pp} is heated at a rate proportional to γ_s , and will escape after a time proportional to $U_{pp}/\gamma_s E_R \propto \Delta/T$. Other loss processes that we expect to contribute are optical pumping to the $F=3$ hyperfine ground state, and, at long trapping times, escape in the direction perpendicular to the lattice axis.

An important goal of this work is to evaluate the feasibility of resolved-sideband Raman cooling and quantum-state preparation in a far-off-resonance lattice. Sideband cooling can remove a quantum of vibration every few oscillation periods; to be feasible, this time must be much less than the time required to pick up a quantum of vibration due to all sources of heating. For the lattice parameters explored in Fig. 4, the most rapid rate of increase in \bar{n} occurs immediately after transfer; it is approximately 20, 40, and $\sim 100 \text{ s}^{-1}$ for the three sets of data. At the same time the vibrational oscillation frequencies in the harmonic approximation are 42 and 60 kHz, for lattice depths of $105E_R$ and $209E_R$, respectively. The increase in \bar{n} during an oscillation period thus falls in the range 0.5×10^{-3} to 2×10^{-3} . This favorable combination of time scales suggests that sideband cooling should be feasible.

To assess the feasibility of quantum-state preparation, one must determine the time scale for decay of motional coherences. This issue is only indirectly addressed by our experiment. Raman spectroscopy in near-resonance lattices has

shown Lamb-Dicke suppression of the decay of vibrational coherences, to a value well below the photon scattering rate [1]. This is indeed what one expects for atoms that are close to harmonically bound. For the lattice parameters of Fig. 4, a simple harmonic-oscillator model then gives an estimate $[(kz_0)^2 \gamma_s]^{-1} \sim 10^{-2} \sim 10^{-2} \text{ s}$ for the lifetime of a vibrational coherence, where z_0 is the rms extent of the vibrational ground state. This is two to three orders of magnitude longer than the harmonic-oscillation period, which sets the time scale for Hamiltonian evolution within a potential well, and suggests that coherent control of the center-of-mass motion may be possible. Starting from the vibrational ground state, one might then generate nonclassical states, such as Fock states and squeezed states [3]. More interestingly, the periodic nature of the lattice potential opens up the prospect of preparing and studying entirely new quantum states that extend over more than one lattice potential well. Quantum-state control within a single potential well becomes particularly interesting if means can be found to load a far-off-resonance lattice with high-density atomic samples. An ultimate goal will be to populate a single quantum state of a three-dimensional potential well with more than one atom. If feasible, this will provide a ‘‘pumping mechanism’’ for recent proposals to construct a matter-wave equivalent of the laser [11]. More generally one may hope to study quantum-statistical effects associated with motion in a lattice potential.

The authors thank I. H. Deutsch for helpful discussions. This work was supported by NSF Contract No. PHY-9503259 and by the Joint Services Optical Program.

-
- [1] For a review, see, for example, P. S. Jessen and I. H. Deutsch *Adv. At. Mol. Opt. Phys.* **37**, 95 (1996).
- [2] C. Monroe *et al.*, *Phys. Rev. Lett.* **75**, 4011 (1995); R. Taieb *et al.*, *Phys. Rev. A* **49**, 4876 (1994).
- [3] D. M. Meekhof *et al.*, *Phys. Rev. Lett.* **76**, 1796 (1996), C. Monroe *et al.*, *Science* **272**, 1131 (1996).
- [4] See, for example, C. S. Adams *et al.*, *Phys. Rep.* **240**, 143 (1994).
- [5] F. L. More *et al.*, *Phys. Rev. Lett.* **73**, 2974 (1994).
- [6] M. Ben Dahan *et al.*, *Phys. Rev. Lett.* **76**, 4508 (1996); S. R. Wilkinson *et al.*, *ibid.* **76**, 4512 (1996).
- [7] B. P. Anderson *et al.*, *Phys. Rev. A* **53**, R3727 (1996); T. Müller-Seydlitz, M. Hartl, B. Brezger, H. Hänsel, C. Keller, A. Schnez, R. J. C. Spreeuw, T. Pfau, and J. Mlynek, *Phys. Rev. Lett.* **78**, 1038 (1997).
- [8] L. S. Goldner *et al.*, *Phys. Rev. Lett.* **72**, 997 (1994).
- [9] D. R. Meacher *et al.*, *Phys. Rev. Lett.* **74**, 1958 (1995).
- [10] One standard deviation, combined systematic and statistical.
- [11] H. M. Wiseman and M. J. Collet, *Phys. Lett. A* **202**, 246 (1995); R. J. C. Spreeuw *et al.*, *Europhys. Lett.* **32**, 469 (1995); A. M. Guzman *et al.*, *Phys. Rev. A* **53**, 977 (1996).